6ICEGE
6th International Conference on Earthquake Geotechnical Engineering
1-4 November 2015
Christchurch, New Zealand

Analysis of Seismic Soil–structure Interaction for a High Monumental Tower in Naples (Italy) under a Historical Earthquake

F. de Silva[1], F. Silvestri[2], F. Ceroni[3], M. R. Pecce[4], S. Sica[5]

ABSTRACT

The paper examines the effects of soil-structure interaction on the dynamic behavior of the historical Carmine bell tower in Naples, damaged by the Sannio earthquake in 1456. The brickwork structure is 68m tall, endowed with direct foundations on a deformable deposit of man-made ground and alluvial sands, overlying volcanic tuff. The structural model was calibrated on existing data, the foundation and the geotechnical subsoil model were reconstructed according to recent investigations. Soil-structure interaction was simulated by simplified and advanced approaches, considering the input motion determined through seismic response analyses. The seismic action on the rock outcrop was defined, simulating the 1456 earthquake. Comparing the results of the analyses on the fixed based structure with those of soil–structure system, the effects of the interaction was recognized in terms of elongation of the period, reduction of the damping and increase of structural displacements due to the rigid rotation of the base.

Introduction

An optimized and reliable seismic protection of historical buildings may be pursued by advanced dynamic analyses of the soil–foundation–structure (SFS) system, for which the reference input motion may be the maximum historical earthquake (MHE). The SFS interaction, usually neglected in practice, may be beneficial or detrimental depending on the relative structure/soil stiffness. The case study described in the following is paradigmatic for assessing the effects of SFS interaction on a slender tower founded on soft soils, located in an area where low-frequency strong motion events are expected, just like the MHE considered.

The case study of Carmine Bell Tower

The case study analyzed in the paper is the Carmine Bell Tower (Figure 1a) in the east seashore of Naples. The site is characterized by significant seismic hazard, according to the National seismic hazard map (MPS working group, 2004), drawn in Figure 1b in terms of median peak ground acceleration, PGA, expected on a reference stiff rock outcrop with a return period of 475 yrs. A value of PGA=0.17g is returned for Naples. Located near the market area of the ancient city, the Bell Tower is part of the "Carmine Maggiore" monumental complex, including a church, a monastery and the S.S. Rosario friary (see Figures 1a and 2a).

The Tower was damaged in 1456, when an earthquake (magnitude M_W = 7.2) with epicenter in the Sannio region (Figure 1b), induced a macroseismic intensity I_{MCS}=VIII at Naples.

[1]Phd Student, Università di Napoli Federico II, Napoli, Italy filomena.desilva@unina.it
[2]Full Professor, Università di Napoli Federico II, Napoli, Italy francesco.silvestri@unina.it
[3]Assistant Professor, Università del Sannio, Benevento, Italy ceroni@unisannio.it
[4]Full professor, Università del Sannio, Benevento, Italy pecce@unisannio.it
[5]Assistant Professor, Università del Sannio, Benevento, Italy stefsica@unisannio.it

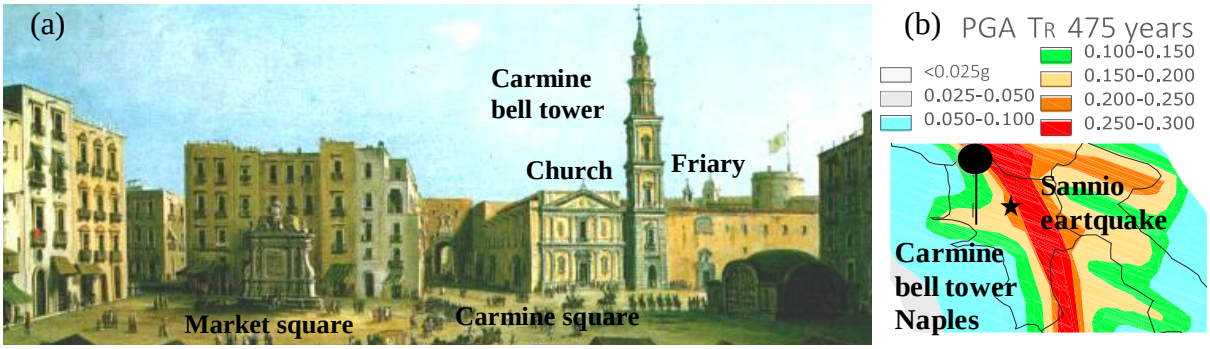

Figure 1.Painting of the Carmine square (a), Naples on the Italian seismic hazard map (b).

The current structure of the Bell Tower, reported in Figure 2, was built on the ancient basement in the XVII century. From the basement up to 41 m, the Tower has a squared cross-section, with faced masonry walls made of yellow tuff. The topmost part has an octagonal cross-section, with clay brick walls with the top covered by a dome. The dynamic identification of the Tower and the mechanical properties of the masonry was detected during a detailed *in-situ* survey (Ceroni et al., 2010). In order to reconstruct the shape and the depth of the foundation, electrical resistivity tomography (ERT) and ground penetrating radar (GPR) survey with boreholes have been recently performed. As reported in Figure 2c-d, the Tower is supported by the E-W main walls which deepen 2 m below the ground level, i.e. at the groundwater level (de Silva et al., 2015).

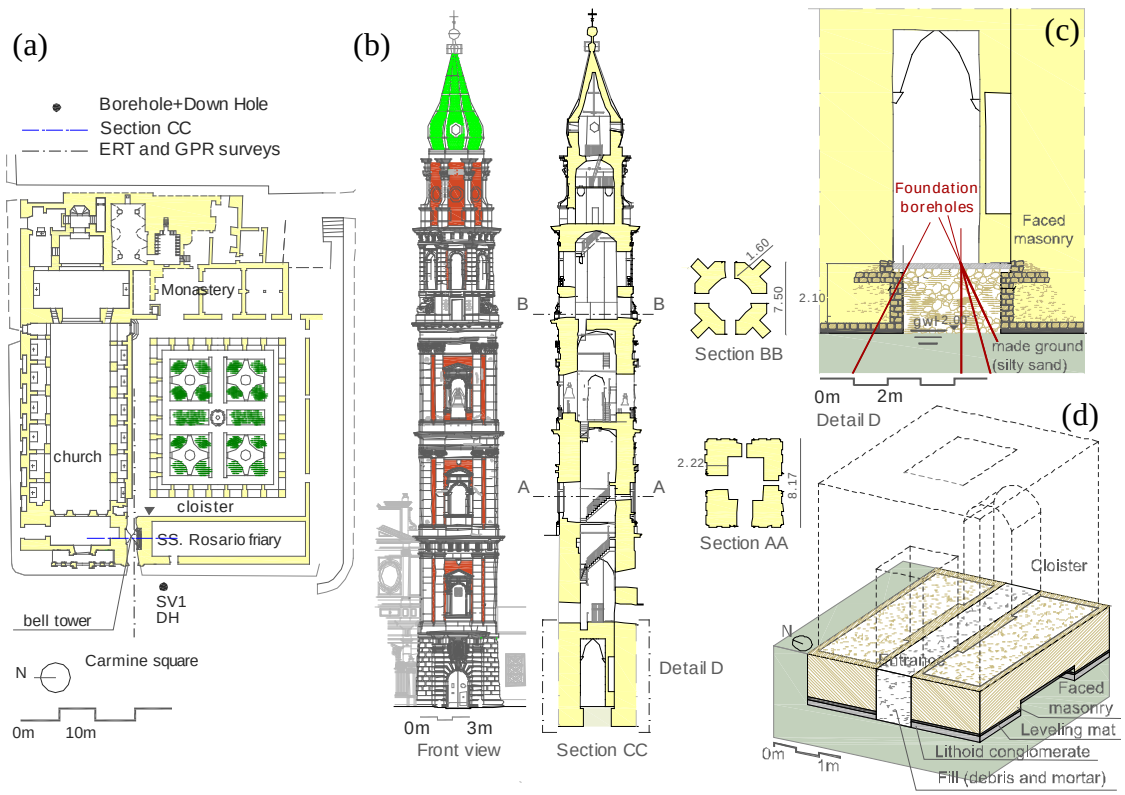

Figure 2. Plan of the investigations in the Carmine monumental complex and square (a); front view and cross sections of the bell tower (b), detail D (c) and 3D reconstruction (d) of the foundation and the surrounding soil.

Subsoil Characterization

A deep borehole was drilled down to a depth of 59 m very close to the external access to the Bell Tower (SV1 in Figure 2a). For the shallowest 3.7 m, the ruins belonging to the ancient Aragonese wall were intercepted. The underlying lithological sequence is quite typical of the Eastern coastal area of Naples (Figure 3a): Man-made Ground (MG) down to 10 m in depth, Marine Sand (MS) interbedded with Pyroclastic Soil (PS) down to 31 m, constituted by volcanic ash lenses and pyroclastic silty sand, 'pozzolana', overlying a layer of lightly cemented Yellow Tuff (YT) followed by Green Tuff (GT) characterized by similar lithological properties.

The water table was intercepted at 2 m depth (Fig. 3a), exactly at the foundation level of the tower. A Down-Hole test was performed in the borehole SV1 (Figure 2a) to measure the compression (V_P) and shear (V_S) wave velocity profiles down to 56m, plotted in Figure 3b. Below the pre-excavation, at depth of 3 m below the ground level, an unusually high value of V_S (500 m/s) corresponds to the Aragonese walls. Thereafter, V_S shows more typical values for cohesionless soils, increasing with depth in the underlying man-made ground, then keeping nearly constant (about 300 m/s) in the upper layer of Marine Sand, except for some minor irregularities in the volcanic ash interbeddings; then grows to 400 m/s at the bottom of the MS-PS formation, where the pyroclastic silty sand is predominant. A significant seismic impedance contrast is detected intercepting the Tuff formation, with values of V_S gradually increasing from 650 m/s at the roof of the YT to 785 m/s in the GT.

Undrained Resonant Column and Torsional Shear tests have been performed on three saturated specimens taken at 12m in the marine sand (MS in Figure 3), 16m and 30m in the pyroclastic soil (respectively PS1 and PS2). The specimens have been consolidated at an isotropic effective stress equal to the mean lithostatic stress, i.e. 70 kPa for MS, 110 kPa and 170 kPa for PS1 and PS2. Figures 3c show the results of the TS tests, in terms of variation of the shear modulus normalized with respect to its initial value, G/G_0 (continuous line), and damping ratio, D (dashed line), as a function of the shear strain, γ. The decay of stiffness and

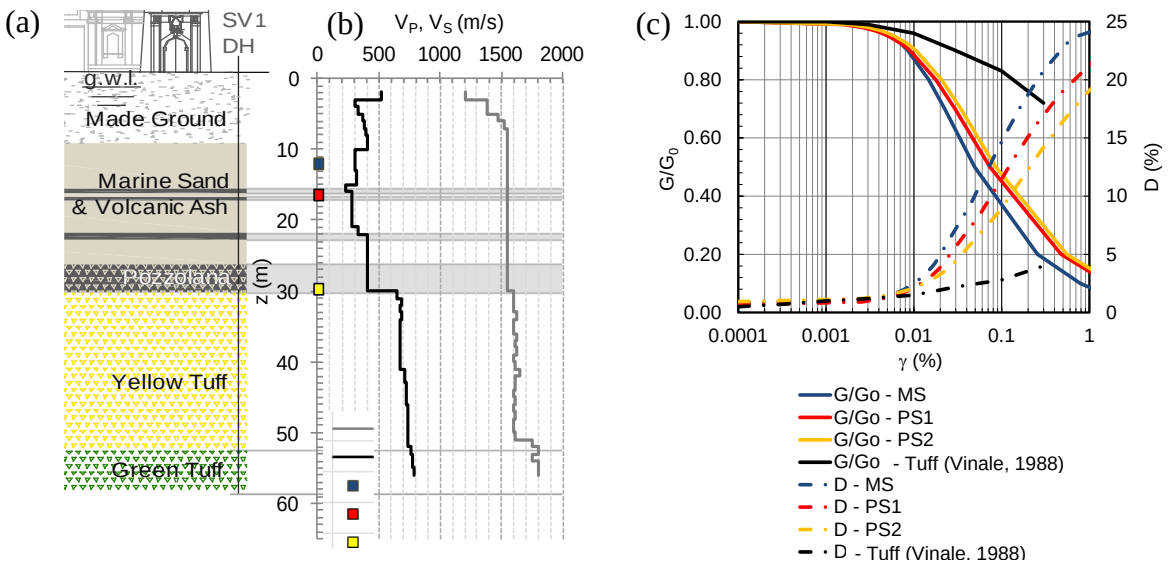

Figure 3. Layering of borehole SV1 (a), V_P and V_S profile resulting from the Down Hole test (b); variation with shear strain, γ, of normalized shear modulus, G/G_0, and damping ratio, D (c).

the increase of damping are comparable for the MS and the PS specimens, whereas the non-linear and dissipative behavior of the pyroclastic soil appears less pronounced when the consolidation stress increases.

Simulation of the Seismic Response to the Historical Earthquake

Although the size and the structure of the destroyed tower were likely different from the current ones, the seismic response of the site was assessed on the basis of the historical earthquake in 1456; this latter was the most destructive ever occurred in Naples, at least according to the Macroseismic Intensity data inferred on the basis of historical chronicles (Rovida et al., 2011). The damage distribution extended across the central-southern Italy, showing maximum values of I_{MCS} as high as XI in three distinct areas, each one of them falling onto different E-W tectonic structures. From this evidence, Fracassi and Valensise (2007) reconstructed a sequence of three main events, with the first (M_W=6.9) occurring on December, 5th, 1456 and generated by the Ariano Irpino (Sannio) fault; both the second (M_W=7.0) and the third (M_W=6.0) shocks occurred on December, 30th, 1456, and were respectively generated by the Frosolone and Tocco Casauria faults (Figure 4a). The 1456 earthquakes caused huge damage in Naples with an overall I_{MCS} = VIII, resulting from the cumulative effects of the Ariano Irpino and Frosolone mainshocks.

The reference maximum acceleration at Naples, PGA_r, was estimated from the felt intensity by two empirical laws suggested by Margottini et al. (1992) and Faenza and Michelini (2010), providing consisting values of 0.19g and 0.21g, respectively. Reference acceleration spectra were estimated as nearly coincident for both mainshocks, through the ground motion prediction equation proposed by Bommer et al. (2003), by assuming a probability of exceedance P_{VR}=10% (red plots in Figure 4b). A set of four accelerograms, recorded on stiff outcrops at comparable source-site distances during recent earthquakes generated by seismogenic zones and mechanisms similar to the historical sequence, was selected from the Italian Accelerometric Archive (http://itaca.mi.ingv.it; Pacor et al., 2011) and scaled to PGA_r=0.18g, provided by the attenuation relationship. The details of the target ground motion and the selected records are shown in Table 1, in terms of source and site characteristics, with indication of the epicentral distance (R), the record peak acceleration (a_{max}), the scaling factor ($SF=PGA_r/a_{max}$), the Pearson coefficient showing the compatibility between the record and target spectral shapes (D_{RMS}) and the Housner Intensity (I_H), which results consistent between the mean scaled records and the target spectrum. The scaling factors are quite high, since the selected records, even if relevant to the strongest instrumental earthquakes belonging to the same seismotectonic areas of the historical sequence in 1456, are characterized by lower M_w than those estimated for the mainshocks.

Figure 4 demonstrates the compatibility between the mean response spectrum of the selected accelerograms (blue plot) and the target spectra within a tolerance range of +0.5σ and -0.35σ (grey area). Both values of a_{max} estimated by the empirical laws (triangles) fall in the tolerance range, with that derived by Margottini et al. (1992) closer to the target peak ground acceleration.

The selected accelerograms were applied as reference input motions at a seismic bedrock assumed coincident with the Green Tuff formation, to carry out one-dimensional seismic response analyses with the EERA code (Bardet et al., 2000). The shear wave velocity model, inferred from the Down Hole test, is shown in Figure 5a. The non-linear and dissipative behaviour of the soils were modelled with the curves shown in Figure 3d, attributing those

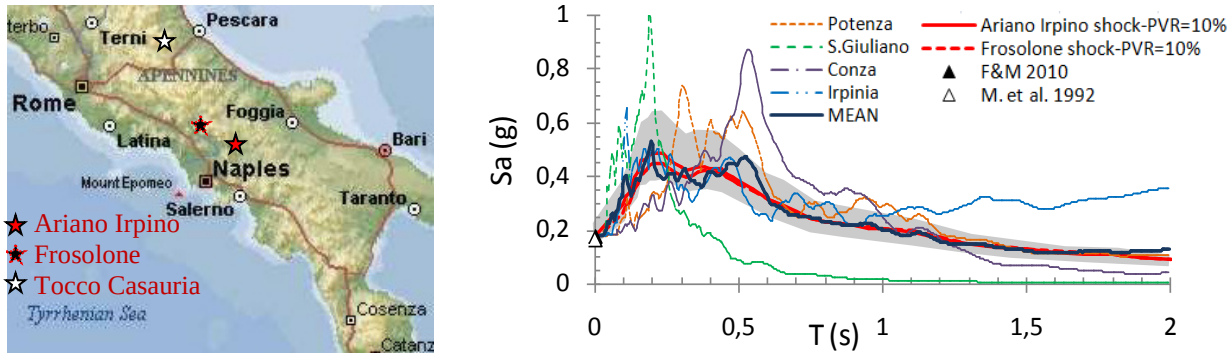

(a) (b)

Figure 4. Epicenters of the three 1456 mainshocks (a), Response spectra of the input motions (b).

Table 1. Comparison between the target and selected events.

Earthquake	Date	M_w	Mechanism	Lenght	Width	Depth	a_{max}	R	SF	D_{RMS}	I_H
				km	km	km	g	km			cm
Ariano Irpino*	5/12/1456	6.9	oblique right-lateral slip	30	15	18	0.18	64	/	/	55
Frosolone*	31/12/1456	7.2		36	15	18	0.18	64	/	/	56
Potenza	05/05/1990	5.8	strike-slip	7.9	6.2	18	0.03	45	6	0.027	62
S.Giuliano	31/10/2002	5.8	right-lateral slip	10.5	8	16	0.03	58	6	0.085	9
Conza	01/12/1980	4.7	/	/	/	/	0.02	79	9	0.058	53
Irpinia	23/11/1980	6.8	normal	28	15	7	0.04	73	4.5	0.066	95
								mean	6.5	0.059	55

*After Fracassi and Valensise, 2007

relevant to the shallowest specimen to the MG formation, and the others to the MS-PS formation, respectively from 10 m to 22 m and from 22 m to 30 m, according to their sampling depth. The curves for the Yellow Tuff were taken from laboratory measurements on the same rock formation (Vinale, 1988). Figure 5b shows the vertical profiles of the maximum acceleration, a_{max}, induced by the selected earthquakes. Across the Yellow tuff, the peak acceleration amplitude increases slowly from 0.12g to 0.15g. The amplitude starts to increase significantly along the marine-pyroclastic sand (MS-PS) formation, reaching a mean value of 0.23g at the top of the sandy layers and 0.27g at the foundation level. The dark grey line in Figure 5c represents the variation of the mean decay of the shear modulus, G/G_0, along the different soil layers above the seismic bedrock. The mobilized shear modulus holds its initial value, G_0, throughout the whole tuff and man made ground formations, indicating a linear behaviour. Non-linear soil behaviour occurs in the MS-PS formation, where the mean peak shear strain reached 0.06%.

Effects of the Compliant Base on the Dynamic Response of the Tower

For studying soil-structure interaction effects, a simplified finite element model of the Tower was developed with the code SAP 2000, by implementing beam elements with squared hollow section varying along the height. The partial interaction with the surrounding buildings was neglected by assuming a cantilever scheme. The first fundamental period of the fixed base tower (FB) was estimated T_0 = 1.93 s by linear modal analysis. In order to investigate soil-foundation-structure interaction, the Bell Tower was first assimilated to a

simple degree of freedom system (SDOF), endowed with the same fundamental period and

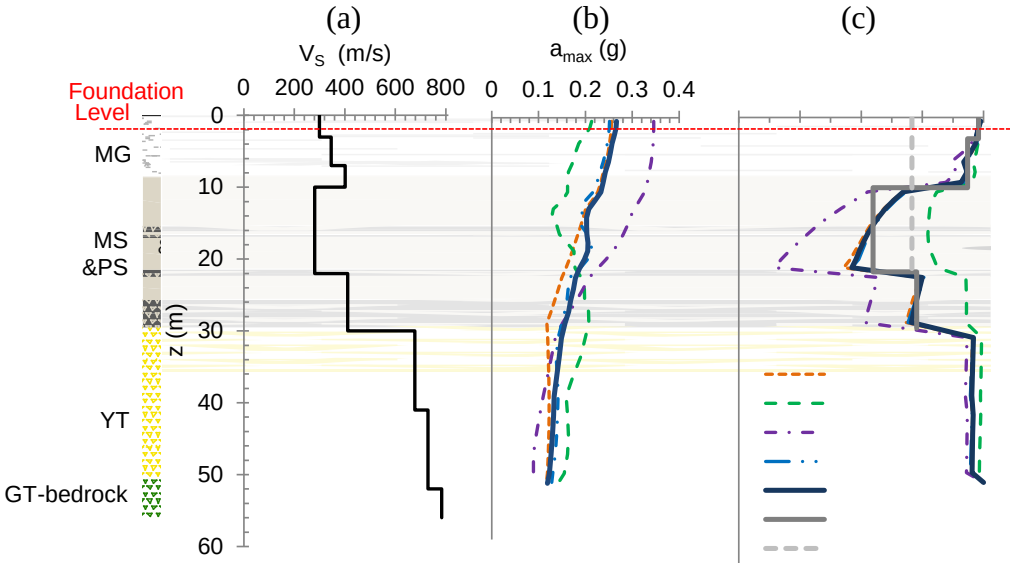

Figure 5. V_S profile inferred from the Down Hole test (a), peak acceleration (b) and mobilized normalized stiffness (c) induced by the reference input motions.

the same lateral stiffness of the fixed-base SAP model, hence with a 'consistent mass' (de Silva et al., 2015). The dynamic impedance of the soil-foundation system was introduced through translational and rotational springs at the SDOF base. The stiffness of the springs was derived by the formulas for an arbitrarily shaped footing provided by Gazetas (1991), conservatively neglecting the embedment. An initial soil stiffness G_0=207 MPa was adopted, cionsistent to an equivalent $V_S \approx$ 330m/s in the first 22 m of the layered soil underneath the foundation level, by assuming a depth equal to twice the foundation width as the soil thickness involved in the interaction (Fig. 5a).

To account for soil non-linearity, the analysis was repeated considering a mobilized shear modulus G_{eq}=191 MPa, according to the mean decay resulting from the seismic response analyses in the uppermost 22 m layering of deformable soils (light grey dashed line in Fig. 5c). The simplified approach proposed by Veletsos and Meek (1974) was applied, calculating the equivalent period, T*, and damping ratio, ξ^*, of the soil-foundation-structure system, in the cases of linear (G_0) and non-linear (G_{eq}) soil behaviour. As expected, the equivalent period increases from the fixed base value (T_0=1.93s) up to T^*=2.21 s, for G_0, and T^*=2.24 s, for G_{eq}. At the same time, the equivalent damping reduced to ξ^*=3.32% (G_0) and to ξ^*=3.22% (G_{eq}), with respect to the usual value, ξ=5%, adopted for fixed-base structures.

Figure 6 shows the mean acceleration spectra resulting from the seismic response analyses at the foundation level (-2.00 m below the ground level) assuming for the structural damping ratio the values ξ=5% (fixed base) and ξ^* (structure with base springs) calculated for G_0 and G_{eq}. For the structure with base springs, the spectral accelerations are slightly variable with respect to the fixed-base case (Sa_{FB}=0.13g, black circle in Fig. 6) in both cases of linear (Sa_{G0}=0.13g, blue rhombus) and non-linear (Sa_{Geq}=0.12g, red triangle) soil behavior, because the decrease of acceleration due to the elongation of the period is counter-balanced by the damping reduction. The soil deformability was also introduced in the SAP model (Figure 7a), equipping the base of the tower with translational and rotational springs with the stiffness previously introduced.

Table 2. Participating mass (M_0, M^*) and periods (T_0, T^*) derived by the modal analyses compared to the simplified approach results, in the fixed base and compliant base cases.

	Modal analyses – SAP model						Veletsos and Meek (1974)		
	Participating mass [%]			Period [s]			Period [s]		
	M_0(FB)	$M^*(G_0)$	$M^*(G_{eq})$	T_0(FB)	$T^*(G_0)$	$T^*(G_{eq})$	T_0(FB)	$T^*(G_0)$	$T^*(G_{eq})$
1st mode	60	54	57	1.93	2.18	2.21	1.93	2.21	2.24
2nd mode	9	12	10	0.48	0.50	0.51	/	/	/
3rd mode	9	10	8	0.27	0.28	0.28	/	/	/

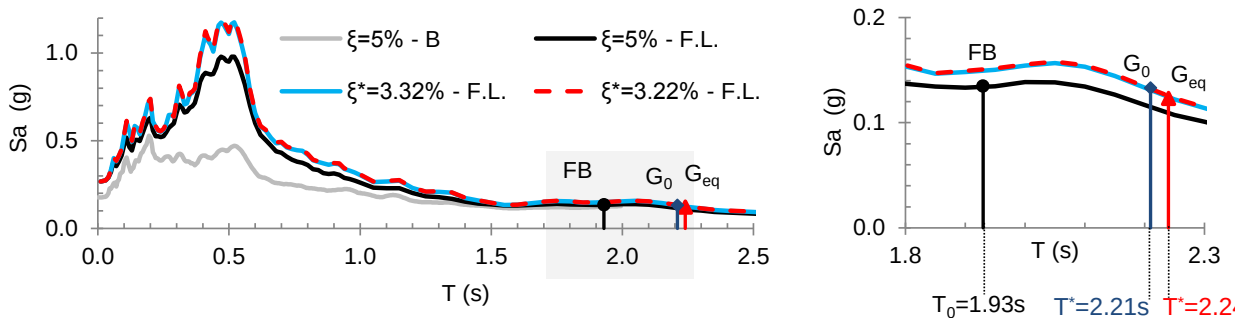

Figure 6. Mean spectra at the Bedrock (ξ= 5% - B) and resulting from seismic response analyses at the Foundation Level, considering ξ= 5% - F.L., ξ^*= 3.15% - F.L. and ξ^*= 3.32% - F.L. (a); zoom on the range of periods of interest for the structure (b).

The elongated periods T* provided by the SAP model are similar to the values provided by the Veletsos and Meek (1974) approach, listed in Table 2. So the simplified approach turns to be reliable, introducing in the replacement oscillator the consistent mass, once the fixed-base period T_0 and the stiffness have been derived from a detailed structural model.

Pseudo-dynamic linear analyses were then executed by combining the effects of the first six vibration modes of the structure, under the seismic action expressed by the spectral acceleration resulting from the seismic response analyses. The reduction in damping caused by the interaction was considered by using the mean acceleration response spectra in Fig. 6 for the cases of:

- fixed-base structure (FB, Fig 7b), loaded by the spectrum with ξ=5% (black line in Fig. 6a);
- structure on base springs with small-strain stiffness (G_0, Fig 7c), loaded by the spectrum with ξ=3.32% (blue line in Fig. 6a);
- structure on base springs with reduced stiffness (G_{eq}, Fig 7c), loaded by the spectrum with ξ=3.22% (red dashed line in Fig. 6a).

As shown in Figure 7b, the total deformation of the tower with the compliant base (u_{SS}) is higher than that computed with the fixed base, and not significantly affected by non-linear soil behaviour. It can be observed that, scaling out the rigid displacements of the tower caused by the base rotation (u_θ), the flexural deformation of the compliant base structure (u_f in Figure 7 c-d) is only slightly reduced with respect to that of the fixed base ($u_{f,FB}$)

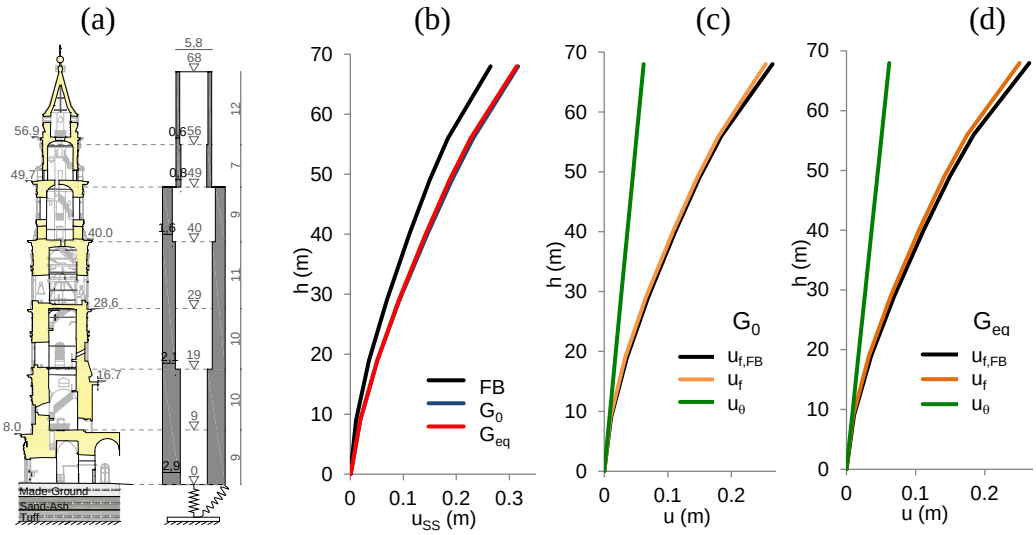

Figure 7. Section and model (a) of the tower; deformed shapes in the FB, G_0, G_{eq}-case (b), total, rigid and flexural displacements considering linear (c) and non-linear (d) soil behavior.

Conclusions

The dynamic behaviour of Carmine bell tower in Naples was assessed, simulating the maximum historical earthquake by seismic response analyses, which highlighted significant amplification of the reference input motion. An increase of the period and a reduction of the damping of the structure-foundation-soil system were recognized with respect to the fixed-base hypothesis. The simplified approach and the finite element analyses predicted equal periods for the soil-structure system, by assimilating the complex model to an equivalent fixed-base oscillator through the consistent mass. The pseudo-dynamic analyses accounting for soil-structure interaction showed significant rigid displacements, commonly neglected in the structural analyses.

Acknowledgments

The research programme was carried out as part of WorkPackage 5 of the Geotechnical Research sub-project in the framework of the research activity funded by Italian Civil Protection through the ReLUIS (University Network of Seismic Engineering Laboratories) Consortium.

References

Bardet JP, Ichii K, Lin C H. *EERA a Computer Program for Equivalent-linear Earthquake site Response Analyses of Layered Soil Deposits.* Univ. of Southern California. Dep. of Civil Eng. 2000

Bommer J J, Douglas J, Strasser F O. *Style-of-Faulting in Ground-Motion Prediction Equations. Bulletin of Earthquake Engineering*. 2003; **1**: 171–203.

Ceroni F, Pecce M, Manfredi G. Seismic Assessment of the Bell Tower of Santa Maria del Carmine: problems and solutions. Journal of Earthquake Engineering. 2010; **14** (1): 30-56.

de Silva F, Ceroni F, Sica S, Pecce M R, Silvestri F. Effects of soil-foundation-structure interaction on the seismic behaviour of monumental towers: the case study of the Carmine Bell Tower in Naples. Rivista Ital. di *Geotecnica, special edition* "Il ruolo della geotecnica nella salvaguardia dei monumenti e dei siti storici", 2015, in press.

Faenza L, Michelini A. Regression analysis of MCS intensity and ground motion parameters in Italy and its application in ShakeMap. *Geophys. Journal International*. 2010; **180**:1138–1152.

Fracassi U, Valansise G. Unveiling the sources of the catastrophic 1456 multiple earthquake Hints to an unexplored tectonic mechanism in southern Italy. BSSA. 2007; **97:**725-748.

Gazetas G. Formulas and charts for impedances of surface and embedded foundations. *Journal of Geotechnical Engineering* **117**: 1363-1381.

Margottini C, Molin D, Serva L. Intensity versus ground motion: a new approach using Italian data, *Engineering Geology*. 1992; **33:** 45-48.

MPS Working Group. *Redazione della mappa di pericolosità sismica prevista dall'Ordinanza PCM 3274 del 20 marzo 2003*. Final report for the Department of Civil Protection, INGV, Milano-Roma, 2004.

Pacor, F, Paolucci R, Luzi R, Sabetta F, Spinelli A, Gorini A, Nicoletti M, Marcucci S, Filippi L, Dolce M, Overview of the Italian strong motion database ITACA 1.0, *Bull Earthquake Eng*. 2011; **9**(6), 1723–1739.

Rovida A, Camassi R, Gasperini P, Stucchi M. CPTI11, the 2011 version of the Parametric Catalogue of Italian Earthquakes. Milano, Bologna. http://emidius.mi.ingv.it/CPTI, DOI: 10.6092/INGV.IT-CPTI11. 2011

Veletsos AS, Meek JW. Dynamic behaviour of building-foundation systems. *Earthquake Engineering and Structural Dynamics*. 1974; **3**:121-138.

Vinale F. Caratterizzazione del sottosuolo di un'area campione di Napoli ai fini della microzonazione sismica. *Rivista Italiana di Geotecnica*. 1988; **22**(3):77-100.